

On the Long-term Deflection Behavior of Timber–concrete Composite Slabs

Mokhtar Tantawi^{1,2*}, Dániel B. Merczel¹, János Lógó¹

¹ Department of Structural Mechanics, Faculty of Civil Engineering, Budapest University of Technology and Economics, Műegyetem rkp. 3., H-1111 Budapest, Hungary

² ARC-S Innovation Technology Ltd., Vörösmarty utca 18., 2233 Ecser, Hungary

* Corresponding author, e-mail: mokhtar.tantawi@edu.bme.hu

Received: 18 October 2025, Accepted: 13 November 2025, Published online: 25 November 2025

Abstract

This paper investigates the long-term behavior of cross-laminated timber (CLT)–concrete composite (TCC) slabs through a large-scale parametric study using a two-layer finite-element model with interface springs to represent partial interaction. The study isolates the influence of four parameters—concrete shrinkage (modeled via relative humidity, RH), composite factor (γ), concrete creep coefficient (φ), and timber creep coefficient (K_{def})—on time-dependent deflections. A total of 36,864 analyses were performed for a 6 m span under quasi-permanent loading, with results normalized to the least-deflecting case in each subset.

For a representative configuration (CLT 120 mm, concrete 50 mm) and RH = 60%, the normalized 50-year deflection increases by approximately 22% with higher shrinkage, by 6% when reducing γ from 0.9 to 0.3, by 8% when increasing φ from 1.5 to 3.0, and by 12% when increasing K_{def} from 0.6 to 1.0. Across configurations, shrinkage is consistently the dominant driver. Moreover, shrinkage-induced deflection scales approximately linearly with the distance from the centroid of the concrete layer to the composite neutral axis (Z_{na}), highlighting geometry as a primary design lever.

The design implications are as follows: 1. prioritize low-shrinkage concrete mixes; 2. avoid intentionally reducing γ , as global stiffness and overall performance deteriorate; and 3. select layer proportions that minimize Z_{na} while balancing the stiffness gains and shrinkage sensitivity associated with thicker concrete toppings.

Keywords

cross-laminated timber, timber-concrete composite, parametric, shrinkage, composite factor

1 Introduction

The use of cross-laminated timber (CLT) slab systems has expanded rapidly across Europe over the past decade [1, 2]. Both manufacturers and researchers are striving to develop efficient and economically viable solutions for large-scale timber construction [3, 4]. CLT consists of layers of sawn timber boards bonded together with alternating grain orientations, resulting in panels that exhibit improved strength and dimensional stability in both directions compared to solid timber [5]. This material offers several advantages, including a reduced carbon footprint, a high strength-to-weight ratio, and faster construction times [5–8]. Since timber weighs only about one-fifth as much as concrete, CLT is particularly attractive for vertical extensions of existing or historical buildings [9, 10]. However, CLT structures can be more sensitive

to vibrations than conventional concrete systems, and the unit cost of timber remains comparatively higher [11].

A widely adopted approach to overcoming these limitations is the use of timber–concrete composite (TCC) systems, which combine a CLT slab with a concrete topping to achieve higher stiffness, improved acoustic and fire performance, and enhanced vibration control [1, 12, 13]. The connection between the two layers may be provided by screws, notches, or epoxy adhesives, each offering different degrees of composite action [2, 14, 15]. The efficiency of the interface is quantified by the composite factor (γ) defined in Eurocode 5 [16]. A value of $\gamma = 1$ represents full interaction, while $\gamma = 0$ corresponds to no connection [17, 18]. In practice, γ lies between these two extremes, depending on the type of connector. Screw connections

are ductile but provide moderate stiffness. Notched interfaces achieve high stiffness at the expense of additional prefabrication. Epoxy adhesives deliver the best mechanical bond but are difficult to apply reliably on-site.

Numerous studies have examined the design and behavior of TCC slabs under both ultimate and serviceability limit states [10, 19–21]. Because such systems are typically used for spans between 7 and 11 meters, their design is often governed by serviceability requirements such as deflection and vibration. Short-term deflections can usually be controlled through appropriate selection of total slab thickness, CLT-to-concrete ratio, and connector stiffness [3]. However, long-term deflections are governed by additional time-dependent phenomena. Concrete exhibits faster creep development than timber, resulting in stress redistribution between the two materials and additional interface stresses, which are most pronounced within the first three to seven years of service [6, 22]. Early-age concrete shrinkage also induces internal stresses that increase long-term deflection, while timber remains more sensitive to variations in humidity and temperature, causing swelling and shrinkage. Furthermore, connectors themselves undergo creep, gradually reducing the composite efficiency over time [23–25].

A comprehensive review by Shi et al. [26] summarizes the state of research on the long-term behavior of TCC structures, categorizing previous work into experimental and numerical investigations. Among the experimental studies, Fragiaco et al. [27] conducted a detailed investigation on wood–concrete composite beams with notched (shear-key) connections. Their 133-day experimental test, supported by long-term numerical extrapolation to 50 years, demonstrated that rheological effects—particularly concrete creep and shrinkage—significantly increase long-term deflections, while stress variations remain relatively minor. They concluded that connection stiffness and environmental humidity are crucial factors in determining serviceability performance. Yeoh et al. [25] conducted a four-year study on 8 m-span laminated veneer lumber (LVL)–concrete composite beams subjected to sustained loading under fluctuating indoor humidity. Deflections were found to be highly sensitive to environmental changes; low temperatures and high humidity increased moisture content and deformation. Beams cast with low-shrinkage concrete showed about 14 percent smaller long-term deflections than those with normal concrete, although all specimens exceeded the span-to-depth ratio limit of 1:200 when extrapolated to a 50-year service life. The authors identified mechano-sorptive effects, concrete

shrinkage, and connector creep as the primary drivers of long-term deformation under cyclic humidity conditions.

Hailu [28] tested four TCC beams under sustained loading in a controlled environment and analyzed the effect of cyclic relative-humidity changes on deflection. An increase in relative humidity (except during the first cycle) reduced deflection, whereas a decrease produced the opposite effect. In contrast, Czabak and Perkowski [29] observed that, one year after loading, beam deflections decreased with falling relative humidity and increased with rising humidity—results that diverged from those reported by Hailu [28].

On the numerical side, Fragiaco et al. [30] developed a three-dimensional model to simulate the long-term behavior of TCC structures, considering environmental variations, concrete shrinkage, and various construction methods. Their results indicated that longer concrete curing times reduce long-term deflections, suggesting that prefabricated concrete toppings can enhance performance. They also demonstrated that temporary shoring of the timber beam offers limited benefits in reducing deflections caused by concrete shrinkage. Binder et al. [31] employed a hybrid analysis approach integrating time-dependent material models to assess load redistribution and deflection development. Their findings revealed that composite slabs deform more than pure CLT slabs but less than reinforced-concrete slabs. While the 3-D model achieved higher accuracy than simplified 1-D models, it required substantially greater computational time; nevertheless, its advantage lay in eliminating the need for experimentally determined slip-modulus data.

Overall, the existing literature on long-term TCC behavior has primarily focused on the constitutive modeling of material creep in wood and concrete. However, the time-dependent slip behavior of shear connectors is often simplified, and the correlation between connector slip and global long-term deformation remains insufficiently understood. Strengthening this link is crucial for enhancing both predictive modeling and practical design guidance for CLT–concrete composite slabs [26, 31].

The goal of this paper is to investigate the influence of various kinematic parameters on the long-term behavior of TCC slabs through a comprehensive parametric study. The study aims to identify the long-term variables that have the most significant impact on structural performance and those of lesser importance, and to provide practical design recommendations for achieving efficient and cost-effective composite slab systems.

2 Methods

2.1 Investigated parameters

Based on the findings from the literature review and practical experience in construction, several parameters were identified as critical to the long-term behavior of TCC slabs. Therefore, the primary objective of this paper is to conduct a comprehensive parametric study to quantify the influence of these parameters and determine the extent to which each affects the long-term performance of TCC slabs. The parameters selected for investigation are:

- creep of concrete,
- creep of timber,
- shrinkage of concrete, and
- the composite factor.

Sections 2.1.1–2.1.5 describe the long-term behavior associated with each of these parameters individually.

2.1.1 Creep of concrete (ϕ)

When structural systems are subjected to sustained loads over time, their deformations gradually increase—a phenomenon known as creep deformation. According to Eurocode 2, both creep and shrinkage are time-dependent properties of concrete, and their effects should generally be considered in the verification of serviceability limit states [32]. The standard specifies that creep and shrinkage depend on several parameters, including relative humidity, the dimensions of the structural element, and the type of cement used. In addition, creep is influenced by the maturity of the concrete at the time the load is first applied. Based on these factors, the final concrete creep coefficient, denoted as $\phi_0(\infty, t_0)$, can be calculated using the formulations provided in Section 3.1.4 of CEN EN 1992-1-1:2004 [32]. For long-term analysis, the effective modulus of elasticity (MoE) of concrete can be reduced to account for the effects of creep relaxation.

2.1.2 Creep of timber (K_{def})

Just like concrete, timber also undergoes creep over time. The magnitude of timber creep depends primarily on environmental exposure conditions. Several models have been developed in the literature to describe the time-dependent behavior of timber, with one of the most widely recognized being Toratti's model [33]. This model separates the long-term deformation of timber into seven components: elastic deformation, viscoelastic creep, strain due to changes in moisture content, mechano-sorptive creep, shrinkage or swelling effects, hygro-expansion strain, and thermal strain [26, 33].

In design practice, a simplified approach is adopted in Eurocode 5 [16], which introduces the deformation modification factor K_{def} to account for time-dependent effects. Although the code does not explicitly define the creep behavior of timber, this factor represents the combined influence of all long-term deformations resulting from sustained loading, moisture content, and variations in moisture. Different service classes are defined according to the expected ambient temperature and relative humidity:

- Service class 1 is characterized by a moisture content corresponding to a temperature of 20 °C and a relative humidity of the surrounding air that only exceeds 65% for a few weeks per year.
- Service class 2 corresponds to a temperature of 20 °C and a relative humidity that only exceeds 85% for a few weeks per year.
- Service class 3 is characterized by climatic conditions leading to higher moisture contents than in service class 2.

Based on these service classes, Eurocode 5 specifies K_{def} values for various timber elements. For CLT, the values of K_{def} are 0.6, 0.8, and 2.0 for service classes 1, 2, and 3, respectively. The MoE of timber is reduced by these factors when assessing long-term performance.

A mathematical power-law relationship is often used to describe the time-dependent creep of timber [34]. To apply this model with reasonable accuracy, it is assumed that both relative humidity and temperature exhibit only small fluctuations over time—an assumption valid for service classes 1 and 2, which generally represent indoor environments. Fig. 1 illustrates a comparison between the creep behavior of timber and concrete.

2.1.3 Shrinkage of concrete (ϵ_{cs})

When materials harden due to chemical reactions or interact with the environment by releasing or absorbing moisture, their volume changes over time. In the case of

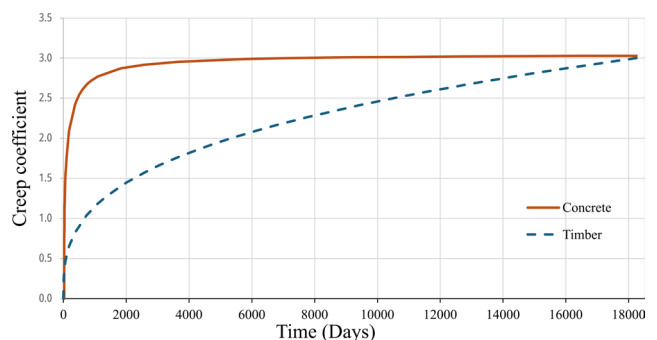


Fig. 1 Creep of timber vs. concrete

concrete, the loss of moisture after hardening leads to a reduction in volume, known as shrinkage. According to Eurocode 2 (CEN EN 1992-1-1:2004) [32], the total shrinkage strain consists of two components: drying shrinkage and autogenous shrinkage.

The total shrinkage strain can be expressed as

$$\varepsilon_{cs} = \varepsilon_{cd} + \varepsilon_{ca}, \quad (1)$$

where:

- ε_{cs} is the total shrinkage strain,
- ε_{cd} is the drying shrinkage strain,
- ε_{ca} is the autogenous shrinkage strain.

Similar to creep, shrinkage develops progressively over time and is affected by several parameters, including the type of cement, the relative humidity of the environment, and the dimensions of the structural element. The evolution of concrete shrinkage over time can be illustrated as shown in Fig. 2.

2.1.4 Psi factor (ψ)

It is well established that concrete and timber exhibit different creep behaviors. If the two materials were to deform independently—without any interaction or restraint between them—the MoE of each material could be considered separately without modification. However, as demonstrated in analytical studies presented in the COST Report [6], when timber and concrete are mechanically connected to form a composite system, it becomes necessary to distinguish between the material creep coefficient and the system creep coefficient.

To account for this interaction, the psi factor (ψ) was introduced. This factor is used to determine the reduced modulus of elasticity of each material in the composite system, reflecting the combined effects of creep interaction between timber and concrete. Values for the ψ factor can be taken from Table 13 in [6].

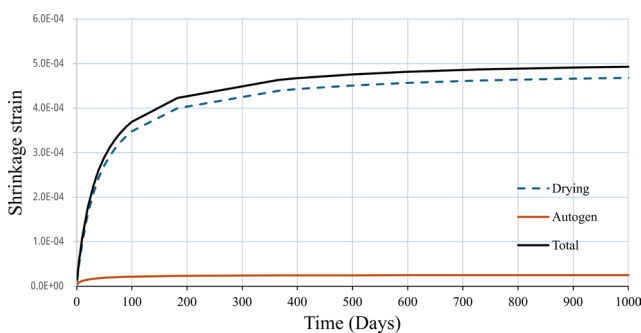


Fig. 2 Shrinkage development in time

2.1.5 Connection efficiency (γ)

As mentioned earlier, the gamma factor (γ) represents the degree of connection efficiency between the concrete and timber layers in TCC systems. Previous research has investigated the range of connector stiffness values required to achieve an efficient level of composite action, suggesting both upper and lower threshold limits for design [17].

In the present study, this investigation is extended to evaluate how variations in connection stiffness—and their creep over time—influence the long-term behavior of TCC slabs, with particular emphasis on their time-dependent deflection performance. The time-dependent behavior of the connectors was accounted for using the K_{def} factor recommended in Eurocode 5 and the reduction factor ψ as specified in Table 13 of [6].

2.2 Numerical study

2.2.1 Two-layer finite element model

Although several finite element (FE) software packages support the design of CLT elements, only a few offer specialized capabilities for modeling CLT–concrete composite systems. AXIS VM, for example, includes a CLT module based on Mindlin plate theory, which is the two-dimensional extension of Timoshenko beam theory [35]. While this approach yields reliable results for CLT slabs, the software [36] does not include dedicated functionality for CLT–concrete composites.

To overcome this limitation, the concrete and CLT layers were modeled separately and coupled through interface elements. Both layers were represented using shell elements, with a mesh composed of six-noded serendipity elements averaging 0.25 m in size. The layers were linked by spring elements, whose stiffness values were defined according to the mechanical properties of the shear connectors. Rotational stiffness was set to zero, and vertical stiffness was given an infinite value to represent the full contact between the layers. The slip stiffness value was defined based on the mechanical properties of the connections, ensuring the partial interaction.

The concrete was modeled as a linear-elastic, isotropic material, while the CLT was treated as a linear-elastic, orthotropic material to capture its directional stiffness characteristics. A linear static analysis was then performed. The modeling approach has been validated in earlier studies and serves as a reliable basis for the present investigation [17].

2.2.2 Settings and variables of the parametric study

The variables considered in the analysis were introduced in Section 2.1, while their numerical values and settings are summarized in Table 1. Deflection responses were evaluated under the quasi-permanent load combination at multiple time intervals throughout the structure's service life, extending up to 50 years. The study considered slab configurations that were either simply supported or continuous over two or three spans. However, the scope of this paper is limited to the results obtained for the simply supported slabs where one support was a pinned connection and the other was a roller. The time of loading on the composite slab was 28 days, when the concrete had fully cured.

Owing to the large number of variable combinations and time steps required, a total of 36,864 linear static analysis runs were performed. This extensive parametric study was automated through a custom loop developed in Rhino Grasshopper, which interfaced directly with AXIS VM to generate and execute the individual analysis runs.

Table 1 Material and load parameters

Parameter	Values
Creep coefficient of concrete (ϕ)	1.5 – 2 – 2.5 – 3
Creep coefficient of timber (K_{def}) ¹	0.6 – 0.8 – 1
Shrinkage of concrete (RH) ^{2,3}	60% – 70% – 80% – 90%
Gamma factor (γ)	0.3 – 0.65 – 0.9
Span (m)	6
Dead loads (kN/m ²)	1
Live loads (kN/m ²)	1
Unit-weight (kg/m ³)	CLT: 450. Concrete: 2500
Concrete thickness (mm)	50 – 70 – 80
CLT thickness (mm)	100 – 120 – 150 – 180 – 200 – 240
Timber quality	C24. MoE = 11,000 N/mm ²
Concrete quality	C20/25–X0–16–F2. MoE: 30,000 N/mm ²

1. Since the analyses were performed under indoor environmental conditions, the values of K_{def} used were 0.6 and 0.8, corresponding to service classes 1 and 2, respectively. A value of 1.0 was also included, although it does not correspond to a specific service class; it was introduced to allow proportional scaling of the timber's MoE based on K_{def} .

2. The shrinkage of concrete was modeled as an equivalent thermal load applied to the surface of the concrete layer, following the approach described in [24].

3. The shrinkage of concrete was evaluated in terms of relative humidity (RH) to facilitate comparison between cases. It is important to note that RH affects both the creep of concrete and timber, as well as the shrinkage of concrete. However, to isolate the individual effects of each variable for clearer comparison, RH in this study—and throughout the remainder of the paper—is considered only in relation to concrete shrinkage.

3 Results and discussion

Data points exported from the parametric study were processed and will be presented in Section 3, broken down into several segments for easier understanding of the results.

3.1 Long-term effects

Figs. 3–6 present the long-term deflection behavior of the composite slab with a configuration of CLT = 120 mm (5-ply) and a concrete topping of 50 mm. The overall response exhibits a rapid increase in deflection during the initial five years, followed by a gradual, quasi-linear growth over the following decades.

Fig. 3 illustrates the influence of concrete shrinkage, represented here by varying RH levels. As expected, a reduction in RH (corresponding to higher shrinkage strains) results in larger long-term deflections. This trend is consistent with previous findings reported in the literature [13, 24, 37].

Fig. 4 shows the effect of the composite factor, which characterizes the degree of interaction between the CLT and the concrete layer. It can be observed that increasing the composite efficiency reduces global deflections, as a higher γ value implies a stiffer composite action and reduced slip at the interface. This is also in agreement with prior studies [17, 20].

Figs. 5 and 6 highlight the influence of creep effects in concrete ϕ and timber K_{def} , respectively. In both cases, larger creep coefficients lead to increased deflections over time, reflecting the time-dependent stiffness reduction of each material.

To better understand and quantify the influence of each variable on the deflections, each deflection curve in Figs. 3–6 is normalized to the curve with the minimum deflection. For example, in Fig. 3, all curves are normalized to the RH = 0.9 curve, which represents the case with the least deflection.

Among all long-term effects considered, concrete shrinkage appears to have the most pronounced influence on total deflection. This observation supports the conclusions of previous research [6, 20, 25, 38]. Figs. 7–10 present the corresponding normalized deflection curves for the same slab configuration (120 – 5s + 50 mm), further illustrating the system's relative sensitivity to each long-term parameter.

Fig. 7 shows that as shrinkage loads increase, the total long-term deflections can rise by approximately 22% for the case of RH = 60% in the examined slab configuration. Fig. 8 shows that reducing the composite factor from $\gamma = 0.9$ to $\gamma = 0.3$ results in about 6% higher deflections.

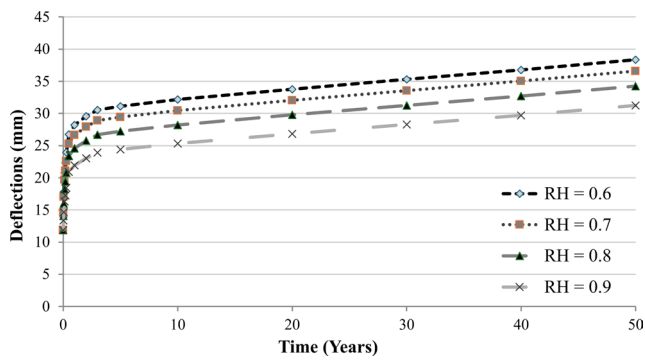


Fig. 3 Deflections of 120 - 5s + 50 mm (Shrinkage)

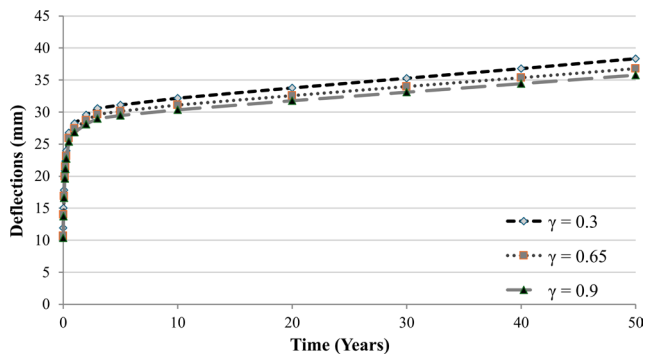


Fig. 4 Deflections of 120 - 5s + 50 mm (γ)

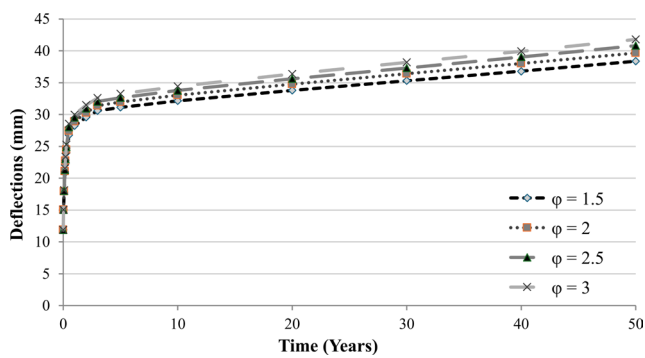


Fig. 5 Deflections of 120 - 5s + 50 mm (ϕ)

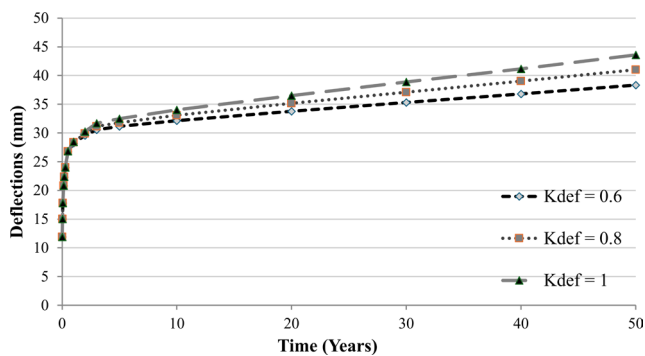


Fig. 6 Deflections of 120 - 5s + 50 mm (K_{def})

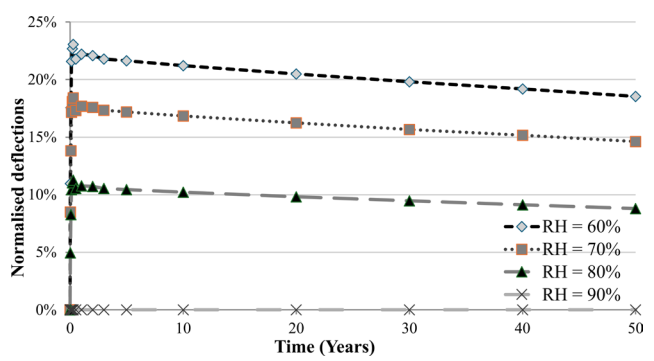


Fig. 7 Normalized deflections of 120 - 5s + 50 mm (Shrinkage)

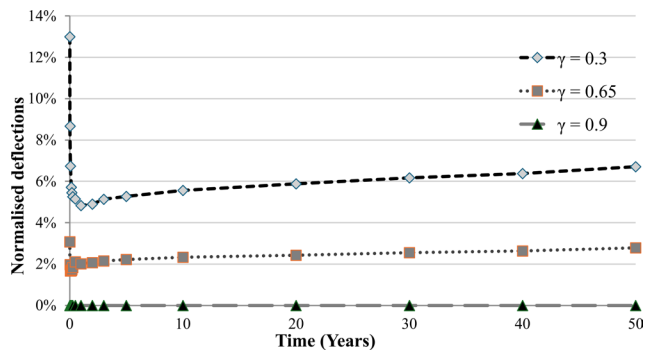


Fig. 8 Normalized deflections of 120 - 5s + 50 mm (γ)

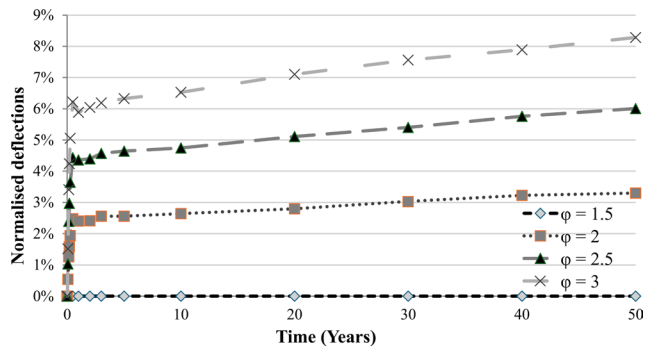


Fig. 9 Normalized deflections of 120 - 5s + 50 mm (ϕ)

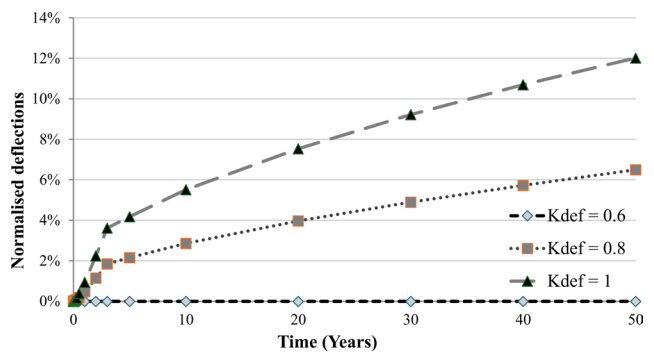


Fig. 10 Normalized deflections of 120 - 5s + 50 mm (K_{def})

In Fig. 9, increasing the concrete creep coefficient from $\phi = 1.5$ to $\phi = 3.0$ leads to an approximate 8% increase in deflection by the end of the 50-year service period. Finally, Fig. 10 indicates that changing the timber creep

coefficient from $K_{def} = 0.6$ to $K_{def} = 1.0$ produces around 12% higher deflections.

It should be noted that these relative increases vary depending on the thickness ratio between the CLT and

the concrete layer. For instance, in configurations with a thicker concrete topping, the contribution of the concrete creep coefficient to the total deflection becomes more significant. Nevertheless, after examining several slab configurations, it was consistently observed that concrete shrinkage remains the most critical long-term parameter influencing deflection. Therefore, Section 3.2 focuses on identifying the parameters that affect shrinkage and exploring how design decisions related to slab geometry—rather than relying solely on low-shrinkage concrete mixtures—can be employed to mitigate shrinkage-induced deflections.

3.2 Factors affecting shrinkage

Since concrete shrinkage was identified as the most significant long-term effect, Section 3.2 examines how the previously introduced parameters interact and influence the overall shrinkage behavior. In the final part, the relationship between shrinkage and the distance from the centroid of the concrete layer to the neutral axis of the composite section is discussed in detail.

3.2.1 Composite factor (γ)

Fig. 11 illustrates the relationship between the composite factor and the corresponding shrinkage-induced deflections. The curves labeled $\gamma = 0.9$ to $\gamma = 0.3$ represent the normalized shrinkage–deflection responses for the case of RH = 60%. It can be observed that as the composite factor increases, the deflections attributed to shrinkage also increase.

This behavior occurs because a higher degree of composite interaction enhances the transfer of shrinkage strains from the concrete layer to the timber substrate. Nevertheless, despite the slightly larger shrinkage-induced deflections at higher γ values, the overall structural performance of the system remains superior, as a higher composite factor results in greater stiffness and reduced total deformation under sustained loading. Therefore, it is not recommended to intentionally design for lower γ

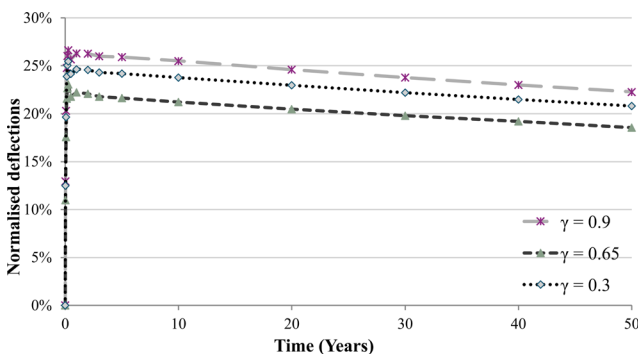


Fig. 11 Shrinkage deflections vs. γ

values, as this would diminish the composite action and adversely affect both stiffness and ultimate capacity [17].

3.2.2 Concrete creep coefficient (ϕ)

The curves shown in Fig. 12 follow the same logic as those presented in Section 3.2.1. They represent the shrinkage–deflection responses for the case of RH = 60%. It can be observed that as ϕ increases, the deflections induced by shrinkage decrease.

This behavior is physically reasonable, since concrete creep leads to stress relaxation within the concrete layer, thereby reducing the internal stresses associated with shrinkage and consequently lowering the resulting deflections.

3.2.3 Timber creep coefficient (K_{def})

Fig. 13 shows that variations in the K_{def} have no significant influence on shrinkage-induced deflections. This indicates that the creep behavior of the timber layer does not significantly interact with the shrinkage effects of the concrete topping, and therefore, its impact on the overall shrinkage response of the composite section can be considered negligible.

3.2.4 Distance from concrete center to neutral axis (Z_{na})

After analyzing the data obtained from the parametric study, it was observed that as the overall cross-sectional thickness increases, the normalized deflection values resulting from

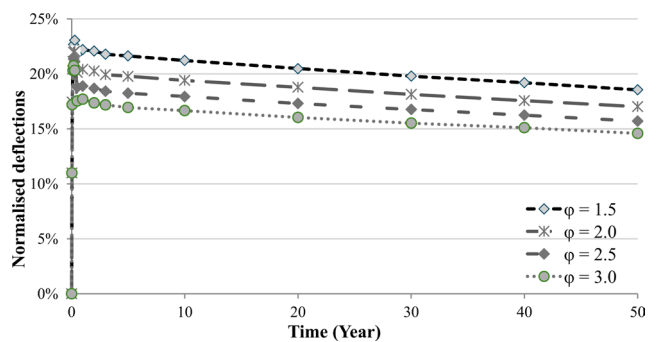


Fig. 12 Shrinkage deflections vs. ϕ

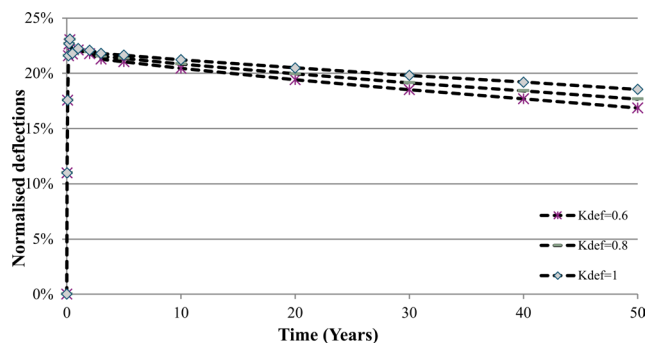


Fig. 13 Shrinkage deflections vs. K_{def}

shrinkage stresses also increase. This trend, however, is not directly related to the thickness of the concrete layer itself.

When comparing two CLT–concrete slab configurations with the same total thickness but different concrete-to-CLT thickness ratios, the shrinkage-induced deflections remain nearly identical (see Figs. 14 and 15).

In contrast, when the total thickness of the composite section is increased, the normalized shrinkage deflections also rise. This can be attributed to the increased distance between the neutral axis of the composite section and the centroid of the concrete layer. A larger separation between these two reference points amplifies the internal moment generated by shrinkage stresses, resulting in higher global deflections.

Fig. 16 presents the relationship between the normalized deflection value at the end of the service life—when both timber and concrete creep have reached their peak and shrinkage is at its maximum—and the distance from the centroid of the concrete layer to the neutral axis of the composite section for several slab configurations. A clear proportional relationship is observed, indicating that the geometry of the composite cross-section has a significant influence on the magnitude of shrinkage-induced deflections.

4 Conclusions

The analyses demonstrated how each investigated parameter influences the overall behavior of the composite slab

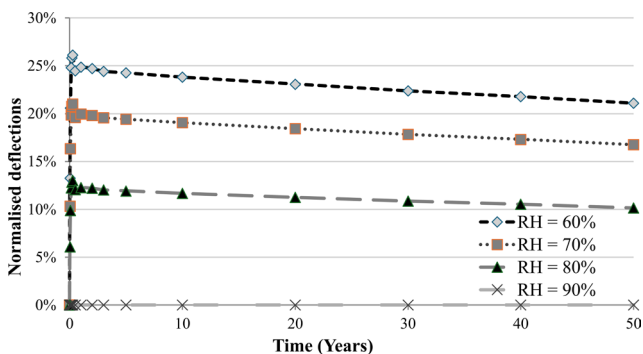


Fig. 14 Shrinkage induced-deflections of 120 – 3s + 80 mm

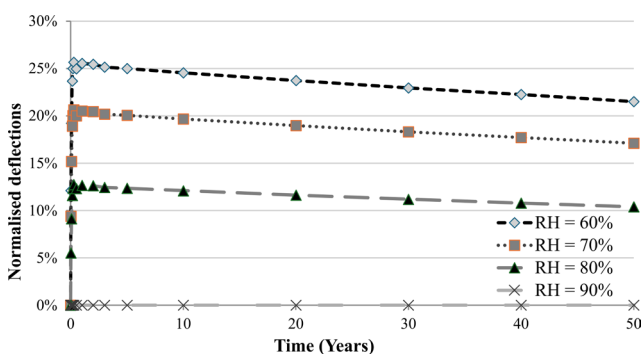


Fig. 15 Shrinkage induced-deflections of 150 – 5s + 50 mm

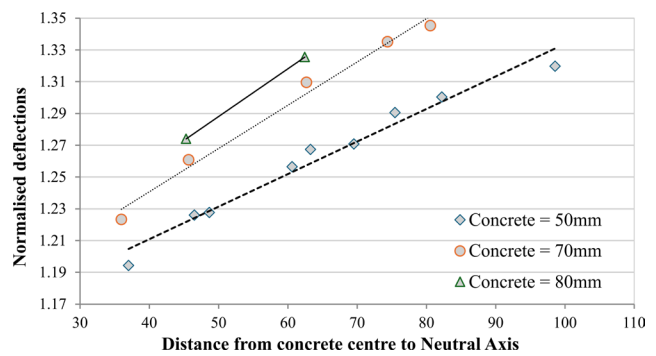


Fig. 16 Relationship between shrinkage-imposed deflections and distance from concrete center to Neutral Axis

configuration, with shrinkage identified as the most critical factor. Subsequently, the interaction between these parameters and their influence on shrinkage-induced deflections was examined in detail. Based on these findings, several design-oriented recommendations are proposed to achieve optimal long-term performance of CLT–concrete composite slabs.

As discussed in Section 3.2.4, the relationship between the distance from the centroid of the concrete layer and the neutral axis and the shrinkage-induced deflections exhibits an approximately linear correlation, where a larger distance results in higher deflection values. Therefore, selecting slab geometries and CLT-to-concrete thickness ratios that minimize this distance can effectively reduce maximum shrinkage-induced deflections.

At the same time, even when two slab configurations share the same Z_{na} value, increasing the thickness of the concrete layer tends to increase shrinkage-induced deflections, although the overall stiffness of the slab becomes higher. Designers should carefully evaluate this trade-off, as thicker concrete layers do not necessarily yield a more optimal long-term design.

It is not recommended to design for a lower composite factor (γ), even though this would slightly reduce shrinkage-induced deflections, because a lower γ leads to a considerable reduction in the overall stiffness of the composite cross-section. Similarly, although a relationship between concrete creep and shrinkage has been observed, increasing the concrete creep coefficient to achieve smaller shrinkage stresses is counterproductive, as the resulting stiffness reduction over the service life would negate any benefit.

Furthermore, there appears to be no direct interaction between the creep behavior of the timber layer and the shrinkage response of the composite system. Therefore, modifying the timber creep coefficient has a negligible influence on shrinkage-related deflections.

To summarize, it is recommended to prioritize low-shrinkage concrete mixtures, as shrinkage was found to be the dominant parameter governing long-term deflections. In addition, designers should aim to select slab configurations that minimize the distance between the neutral axis and the centroid of the concrete layer (Z_{na}) while maintaining an appropriate balance between stiffness and shrinkage sensitivity when determining the thickness ratio of the CLT and concrete layers.

References

- [1] Dias, A., Skinner, J., Crews, K., Tannert, T. "Timber-concrete-composites increasing the use of timber in construction", *European Journal of Wood and Wood Products*, 74(3), pp. 443–451, 2016.
<https://doi.org/10.1007/s00107-015-0975-0>
- [2] Bajzecerová, V. "Bending Stiffness of CLT-Concrete Composite Members - Comparison of Simplified Calculation Methods", *Procedia Engineering*, 190, pp. 15–20, 2017.
<https://doi.org/10.1016/j.proeng.2017.05.301>
- [3] Swedish Wood „The CLT Handbook: CLT structures – facts and planning", The Swedish Forest Industries Federation, 2019. ISBN 978-91-983214-4-3
- [4] Schänzlin, J., Dias, A. "Design of Timber-Concrete-Composite Structures", In: *Proceedings of the 4th International Conference on Timber Bridges*, Biel/Bienne, Switzerland, 2022, pp. 369–381. ISBN 9783906878126
<https://doi.org/10.24451/ehwc-6323>
- [5] Siddika, A., Mamun, M. A. A., Aslani, F., Zhuge, Y., Alyousef, R., Hajimohammadi, A. "Cross-laminated timber–concrete composite structural floor system: A state-of-the-art review", *Engineering Failure Analysis*, 130, 105766, 2021.
<https://doi.org/10.1016/j.engfailanal.2021.105766>
- [6] Dias, A., Schänzlin, J., Dietsch, P. „Design of timber-concrete composite structures: A state-of-the-art report by COST Action FP1402/ WG 4", Shaker Verlag, 2018. ISBN 978-3-8440-6145-1
- [7] Moshiri, F. G., Gerber, C., Crews, K. I. "State of the art on Timber Concrete Composite floor", In: *Proceedings of the 25th Biennial Conference of Concrete Institute of Australia*, Perth, Australia, 2011, pp. 1–12.
- [8] Dániel, H., Habashneh, M., Rad, M. M., "Reliability-based numerical analysis of glulam beams reinforced by CFRP plate", *Scientific Reports*, 12(1), 13587, 2022.
<https://doi.org/10.1038/s41598-022-17751-6>
- [9] Kuilen, J. W. G. V. D., Ceccotti, A., Xia, Z., He, M. "Very Tall Wooden Buildings with Cross Laminated Timber", *Procedia Engineering*, 14, pp. 1621–1628, 2011.
<https://doi.org/10.1016/j.proeng.2011.07.204>
- [10] Jiang, Y., Crocetti, R. "CLT-concrete composite floors with notched shear connectors", *Construction and Building Materials*, 195, pp. 127–139, 2019.
<https://doi.org/10.1016/j.conbuildmat.2018.11.066>
- [11] Hamm, P., Richter, A., Winter, S. "Floor vibrations – new results", In: *Proceedings of 11th World Conference on Timber Engineering (WCTE 2010)*, Vol. 4, Trentino, Italy, 2010, pp. 2765–2774. ISBN 978-1-62276-175-3
- [12] Hamm, P., Knöpfle, V., Ruf, J., Bacher, P., Götz, T., "Full Scale Vibration Tests on a Long Span Timber Floor", In: *World Conference on Timber Engineering (WCTE 2023)*, Oslo, Norway, 2023, pp. 1855–1862.
<https://doi.org/10.52202/069179-0245>
- [13] Yeoh, D., Fragiaco, M., De Franceschi, M., Heng Boon, K. "State of the Art on Timber-Concrete Composite Structures: Literature Review", *Journal of Structural Engineering*, 137(10), pp. 1085–1095, 2011.
[https://doi.org/10.1061/\(ASCE\)ST.1943-541X.0000353](https://doi.org/10.1061/(ASCE)ST.1943-541X.0000353)
- [14] Dias, A. M. P. G. "Mechanical behaviour of timber-concrete connections", PhD Thesis, Delft University of Technology, 2005.
- [15] Thai, M. V., Ménard, S., Elachachi, S. M., Galimard, P. "Performance of Notched Connectors for CLT-Concrete Composite Floors", *Buildings*, 10(7), 122, 2020.
<https://doi.org/10.3390/buildings10070122>
- [16] CEN "CEN EN 1995-1-1:2004 Eurocode 5: Design of timber structures - Part 1-1: General - Common rules and rules for buildings", European Committee for Standardization, Brussels, Belgium, 2004.
- [17] Tantawi, M., Merczel, D. B., Lógó, J. "The effect of slip stiffness on the behavior of timber-concrete composite slabs", *Pollack Periodica*, 2025.
<https://doi.org/10.1556/606.2025.01353>
- [18] Rahman, M. T., Ashraf, M., Ghabraie, K., and Subhani, M., "Assessment of Shear Analogy and Timoshenko Method for Analyzing Hybrid CLT under Out-of-plane Loading", *Proceedings of International Structural Engineering and Construction*, 7(2), pp. MAT-17-1–MAT-17-6, 2020.
[https://doi.org/10.14455/ISEC.2020.7\(2\).MAT-17](https://doi.org/10.14455/ISEC.2020.7(2).MAT-17)
- [19] Auclair, S. C., Sorelli, L., Salenikov, A. "A new composite connector for timber-concrete composite structures", *Construction and Building Materials*, 112, pp. 84–92, 2016.
<https://doi.org/10.1016/j.conbuildmat.2016.02.025>
- [20] Ceccotti, A. "Composite concrete-timber structures", *Progress in Structural Engineering and Materials*, 4(3), pp. 264–275, 2002.
<https://doi.org/10.1002/pse.126>
- [21] Grönquist, P., Müller, K., Mönch, S., Frangi, A. "Design of adhesively bonded timber-concrete composites: bondline properties", *Universität Stuttgart*, Stuttgart, Germany, 2023.
<https://doi.org/10.18419/OPUS-13569>
- [22] Fragiaco, M., Lukaszewska, E. "Influence of the Construction Method on the Long-Term Behavior of Timber-Concrete Composite Beams", *Journal of Structural Engineering*, 141(10), 04015013, 2015.
[https://doi.org/10.1061/\(ASCE\)ST.1943-541X.0001247](https://doi.org/10.1061/(ASCE)ST.1943-541X.0001247)

Acknowledgement

Project KDP-IKT-2023-900-II-00000957/0000003 was implemented with support from the Ministry of Culture and Innovation of Hungary, through the National Research, Development and Innovation Fund, financed under the C2316739 and OTKA K138615 programs.

- [23] To, L., Fragiaco, M., Balogh, J., Gutkowski, R. M. "Long-term load test of a wood–concrete composite beam", *Proceedings of the Institution of Civil Engineers - Structures and Buildings*, 164(2), pp. 155–163, 2011.
<https://doi.org/10.1680/stbu.9.00103>
- [24] Fragiaco, M. "Long-Term Behavior of Timber–Concrete Composite Beams. II: Numerical Analysis and Simplified Evaluation", *Journal of Structural Engineering*, 132(1), pp. 23–33, 2006.
[https://doi.org/10.1061/\(ASCE\)0733-9445\(2006\)132:1\(23\)](https://doi.org/10.1061/(ASCE)0733-9445(2006)132:1(23))
- [25] Yeoh, D., Heng Boon, K., Loon, L. Y. "Timber-concrete composite floor beams under 4 years long-term load", *International Journal of Integrated Engineering*, 5(2), pp. 1–7, 2013.
- [26] Shi, B., Zhou, X., Tao, H., Yang, H., Wen, B. "Long-Term Behavior of Timber–Concrete Composite Structures: A Literature Review on Experimental and Numerical Investigations", *Buildings*, 14(6), 1770, 2024.
<https://doi.org/10.3390/buildings14061770>
- [27] Fragiaco, M., Gutkowski, R. M., Balogh, J., Fast, R. S. "Long-Term Behavior of Wood-Concrete Composite Floor/Deck Systems with Shear Key Connection Detail", *Journal of Structural Engineering*, 133(9), pp. 1307–1315, 2007.
[https://doi.org/10.1061/\(ASCE\)0733-9445\(2007\)133:9\(1307\)](https://doi.org/10.1061/(ASCE)0733-9445(2007)133:9(1307))
- [28] Hailu, M. „Long-term performance of timber-concrete composite flooring systems", MSc Thesis, University of Technology Sydney, 2015.
- [29] Czabak, M., Perkowski, Z. "Experimental investigations of wooden and concrete composite beams subject to long-term load", *MATEC Web of Conferences*, 174, 01016, 2018.
<https://doi.org/10.1051/mateconf/201817401016>
- [30] Fragiaco, M., Balogh, J., To, L., Gutkowski, R. M. "Three-Dimensional Modeling of Long-Term Structural Behavior of Wood-Concrete Composite Beams", *Journal of Structural Engineering*, 140(8), A4014006, 2014.
[https://doi.org/10.1061/\(ASCE\)ST.1943-541X.0000909](https://doi.org/10.1061/(ASCE)ST.1943-541X.0000909)
- [31] Binder, E., Derkowski, W., Bader, T. K. "Development of Creep Deformations during Service Life: A Comparison of CLT and TCC Floor Constructions", *Buildings*, 12(2), 239, 2022.
<https://doi.org/10.3390/buildings12020239>
- [32] CEN „CEN EN 1992-1-1:2004 Eurocode 2: Design of Concrete Structures - Part 1-1: General Rules and Rules for Buildings", European Committee for Standardization, Brussels, Belgium, 2004.
- [33] Toratti, T. "Modelling the creep of timber beams", *Rakenteiden Mekaniikka*, 25(1), pp. 12–35, 1992.
- [34] Morlier, P. „Creep in timber structures", CRC Press, 1994. ISBN 9780429078767
<https://doi.org/10.1201/9781482294750>
- [35] AXISVM "X-LAM (CLT) Theory & Design Guide", Inter-CAD Kft., Budapest, Hungary, 2019.
- [36] Inter-CAD Kft. "AxisVM X8", [computer program] Available at: <https://axisvm.eu> [Accessed: 07 July 2025]
- [37] Khorsandnia, N., Schänzlin, J., Valipour, H., Crews, K. "Time-dependent behaviour of timber–concrete composite members: Numerical verification, sensitivity and influence of material properties", *Construction and Building Materials*, 66, pp. 192–208, 2014.
<https://doi.org/10.1016/j.conbuildmat.2014.05.079>
- [38] Fragiaco, M., Schänzlin, J. "Proposal to Account for Concrete Shrinkage and Environmental Strains in Design of Timber-Concrete Composite Beams", *Journal of Structural Engineering*, 139(1), pp. 162–167, 2013.
[https://doi.org/10.1061/\(ASCE\)ST.1943-541X.0000605](https://doi.org/10.1061/(ASCE)ST.1943-541X.0000605)